Available online at www.sciencedirect.com
ScienceDirect
Journal of Power Sources 160 (2006) 949–956
JOURNAL OF POWER SOURCES
www.elsevier.com/locate/jpowsour

Polymer electrolyte membrane based on 2-acrylamido-2-methyl propanesulfonic acid fabricated by embedded polymerization

Haiqin Pei, Liang Hong, Jim Yang Lee *

Department of Chemical & Biomolecular Engineering, National University of Singapore, 10 Kent Ridge Crescent, Singapore 119260, Singapore

Received 20 December 2005; accepted 1 March 2006
Available online 8 May 2006

Abstract

Methanol crossover through the Nafion membrane is a perennial problem in the operation of direct methanol fuel cells (DMFCs) and therefore justifies the search for a Nafion substitute. This study reports a new methanol-blocking polymer matrix which consists of a methanol barrier phase and an embedded proton source. A three-component polymer blend (TCPB) of poly(4-vinylphenol-co-methyl methacrylate), poly(butyl methacrylate) (PBMA), and Paraloid® B-82 acrylic copolymer resins is used as a methanol barrier. In order to implant a proton source in the membrane as homogeneously as possible, the hydrophilic monomers, 2-acrylamido-2-methyl propanesulfonic acid (AMPS), 2-hydroxyethyl methacrylate (HEMA) and a cross-linking agent (poly(ethylene glycol) dimethylacrylate) (PEGDMA) are polymerized after they have been embedded in the TCPB matrix. The embedded polymerization has resulted in an asymmetric membrane structure, in which the hydrophilic network is sandwiched by two outer layers of predominantly hydrophobic TCPB. Measurements are made of properties of the AMPS-containing membranes that are important to fuel cell applications such as water uptake, ion-exchange capacity, proton conductivity, methanol permeability and tensile strength. The highest proton conductivity of the AMPS-containing membrane is about 0.030 S cm^{-1} at 70 °C. The low methanol permeability (10^{-8} to 10^{-7} cm^2 s^{-1}) of the AMPS-containing membranes is their primary advantage for DMFC applications.

Keywords: Methanol crossover; Fuel cells; Proton conduction; Permeability; Tensile strength; Membrane

1. Introduction

The ability to use a cheap and plentiful fuel (methanol) at relatively low temperatures (ambient conditions) is the major attraction of direct methanol fuel cells (DMFCs) [1,2]. Presently one of the major technical issues impeding the acceptance of DMFCs is the crossover of methanol from the fuel electrode to the air electrode through the proton exchange membrane (PEM). Methanol crossover causes not only fuel losses but also performance losses due to a lowering of the cathode potential and a loss of efficiency in the Pt-based cathode catalyst [3–5]. While poly(perfluorosulfonic acid) (Nafion®) membranes are ubiquitously used in hydrogen fuel cells, they are not appropriate for DMFC applications because of a high rate of methanol crossover. The development of methanol-blocking PEM without significant reduction in proton conductivity and in mechanical properties is a direct solution to the fuel crossover problem.

Incorporating a methanol barrier layer into the Nafion structure is a common strategy to impede methanol crossover through the PEM. The simplest implementation is to deposit a methanol barrier film on the Nafion surface. The barrier film can range from recast polybenzimidazole [6], to Pd [7,8], PVA [9] and polypyrrole composites [10]. The methanol-blocking layer can also be assembled into a multilayered structure. Trilayer membranes consisting of a central methanol barrier layer (Nafion-PVDF) and two external proton-conducting layers were used by Si et al. [11]. Similarly, Yang and Manthiram [12] fabricated multilayer membranes containing a thin central layer of sulfonated poly(ether ether ketone) (PEEK) and two outer layers of recast Nafion. In these approaches, methanol crossover is impeded by increasing the thickness of the blocking layer, which also leads to a concomitant decrease in proton conductivity. Another approach is to use membranes with a dispersed methanol-resistant phase to distribute the methanol-blocking

* Corresponding author. Tel.: +65 6874 2899; fax: +65 6779 1936.
E-mail address: cheleejy@nus.edu.sg (J.Y. Lee).

0378-7753/$ – see front matter © 2006 Elsevier B.V. All rights reserved.
doi:10.1016/j.jpowsour.2006.03.028

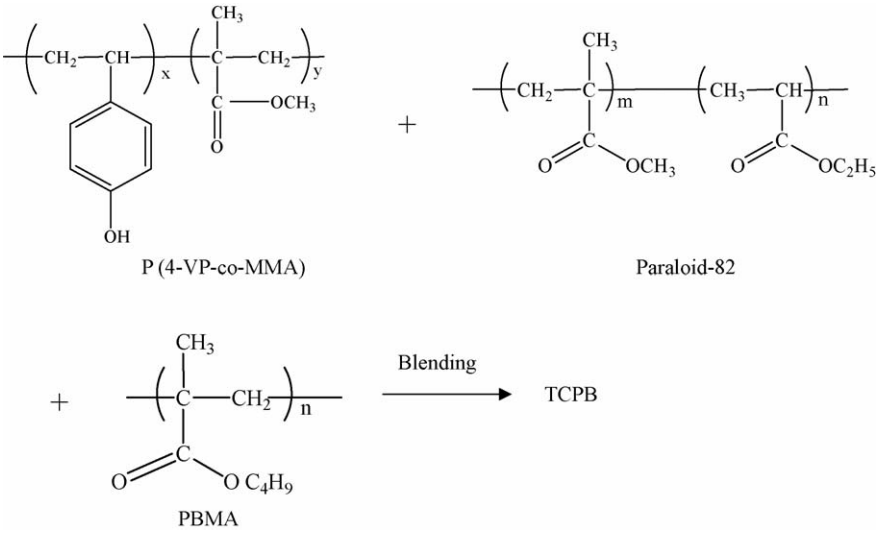

Scheme 1. Chemical component of TCPB.

properties uniformly throughout the membranes while maintaining reasonably good proton conductivity.

In this work, a three-component polymer blend (TCPB) of poly(4-vinylphenol-co-methyl methacrylate) (P(4-VP-MMA)), poly(butyl methacrylate) (PBMA), and Paraloid® B-82 acrylic copolymer resins is used as a methanol-barrier (Scheme 1). The design is based on the low solubility of acrylic polymers in methanol, with Paraloid® B-82 resins and PBMA providing a flexible yet structurally stable framework that is needed for membrane processing. A random copolymer of 2-acrylamido-2-methylpropanesulfonic acid (AMPS) and 2-hydroxyethyl methacrylate (HEMA) is incorporated into the TCPB matrix as the proton source. The hydrophilic 4-VP segments in P(4-VP-MMA) (18.2 wt.%) also take part in forming proton-conducting channels in the TCPB matrix together with AMPS. The choice of AMPS is based on its superior ability to support ion conduction under low water conditions compared with Nafion [13], which is an important consideration for fuel cells that operate at high temperatures. The HEMA units are essential for creating a hydrophilic environment for the proton-supplying AMPS units (Scheme 2) as well as providing structural stability. An embedded polymerization scheme is used to circumvent the thermodynamic immiscibility between the (AMPS–HEMA) copolymer and TCPB. In this procedure, AMPS and HEMA, as well as poly(ethylene glycol) dimethylacrylate (PEGDMA), an oligomeric cross-linking agent is used to form a hydrophilic network that percolates throughout the TCPB matrix. The free-radical copolymerization of AMPS, HEMA and the cross-linking agent occurs only after the evaporation of the volatile components in the mixed solvent system during membrane processing. The product is a homogeneous and free-standing membrane. This paper provides a detailed account of the fabrication process, and reports several properties of the membrane that are relevant to DMFC applications, namely: water uptake, ion-exchange capacity (IEC), proton conductivity, methanol permeability, and tensile strength.

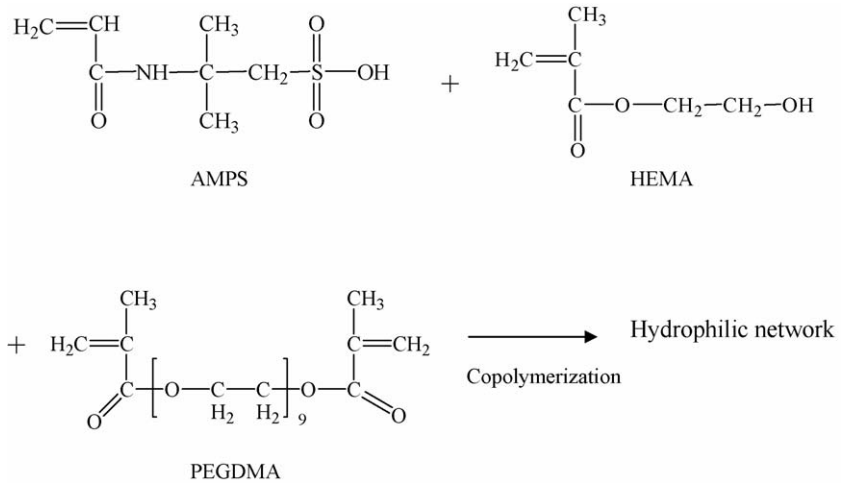

Scheme 2. Chemical structures of (AMPS–HEMA) and PEGDMA cross-linking agent.

2. Experimental

2.1. Materials

2-Acrylamido-2-methyl propanesulfonic acid (AMPS), poly(4-vinylphenol-co-methyl methacrylate) (51 mol% 4-VP), poly(butyl methacrylate) (average $M_w = 337{,}000$), methyl ethyl ketone (MEK), *N*,*N*-dimethylformamide (DMF) (HPLC grade), 1-butanol (99.8%, HPLC grade), benzyl peroxide (BPO) were all obtained from Aldrich, while sodium chloride and sodium hydroxide were obtained from Merck. All the materials were used without purification. Paraloid® B-82 acrylic copolymer resins (56.1 wt.% methyl methacrylate and 43.9 wt.% ethyl acrylate) were supplied by Rohm & Haas. 2-Hydroxyethyl methacrylate (HEMA), poly(ethylene glycol) dimethylacrylate ($M_w = 550$) from Aldrich were used for copolymerization after the removal of the hydroquinone (HQ) inhibitor by an inhibitor removal column provided by Aldrich. Nafion®117 films (equivalent weight of 1100) for the purpose of comparison were also received from Aldrich.

2.2. Membrane preparation

2.2.1. Solution A

Three hundred milligram of poly(4-vinylphenol-co-methyl methacrylate), poly(butyl methacrylate), and Paraloid® B-82 acrylic copolymer resins (in weight ratio of 1:1.7:0.3) were dissolved in 5 ml MEK. A clear yellowish solution was obtained after stirring for 6 h at room temperature.

2.2.2. Solution B

AMPS, HEMA, PEGDMA and an appropriate amount of the BPO initiator (at 7 wt.% of the total monomer, units) were dissolved in DMF (3 ml) at room temperature to form a clear colourless solution. Solutions with different ratios of the monomer units were formulated (Table 1).

Solutions A and B were mixed and stirred for 12 h at room temperature. The mixture was poured into a Telfon dish and dried at room temperature for 6 h to remove most of the MEK. Further drying was carried out in a nitrogen atmosphere at 100 °C for 24 h. Free-radical polymerization of the embedded monomers (AMPS, HEMA, and PEGDMA) occurred during this drying period. A homogenous free-standing membrane was obtained, which could be easily peeled from the Teflon dish. The flow chart for membrane preparation is given in Scheme 3.

Table 1
Composition of multi-component membranes

Membranes	SO_3H (mmol g^{-1})	TCPB (g)	Solution B[a]		
			AMPS (g)/%	HEMA (g)/%	PEGDMA (g)
AMPS-1	0.35	0.3	0.05/12.8	0.25/64.1	0.09
AMPS-2	0.40	0.3	0.05/15.4	0.20/61.5	0.075
AMPS-3	0.53	0.3	0.08/18.6	0.25/58.1	0.10
AMPS-4	0.61	0.3	0.10/24.2	0.28/56.7	0.114
AMPS-5	0.70	0.3	0.10/25.6	0.20/51.3	0.09

[a] The weight percentage of PEGDMA is kept 23% throughout all the compositions of B.

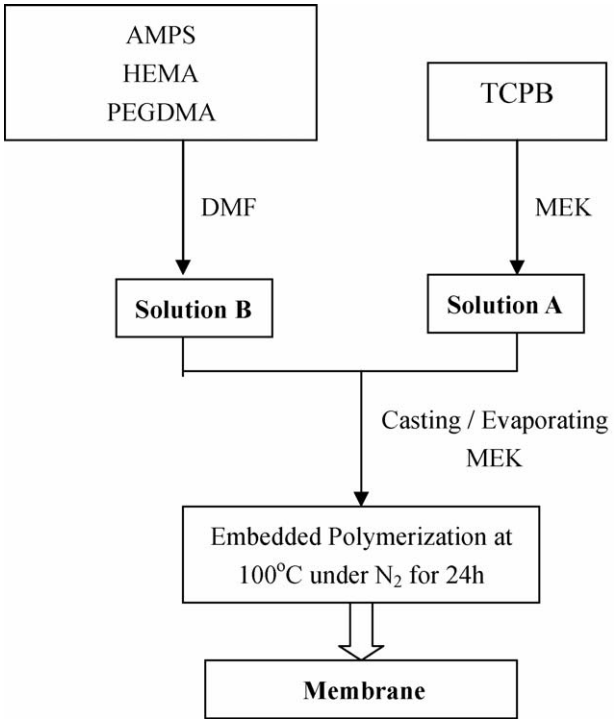

Scheme 3. Flow chart of membrane preparation.

2.3. Membrane characterizations

2.3.1. Membrane morphology

The cross-section of the membrane was examined by field emission scanning electron microscopy (FESEM) using JEOL JSM-6700F instrument operating at 15 kV. The specimens were prepared by freezing the dry membrane samples in liquid nitrogen and then breaking them up to produce a cross-section. Fresh cryogenic fractures of the samples were spray-coated with a thin layer of Pt under vacuum prior to FESEM examination.

2.3.2. Water uptake

The equilibrium water contents in the membranes (various compositions) at room temperature were determined gravimetrically. A membrane after vacuum drying at 70 °C for 24 h was weighed and placed in deionized water for 24 h, at room temperature. The weight was taken again after removal of surface-attached water. Water uptake was calculated from the weight difference as follows:

$$\text{water uptake}\,(\%) = \frac{W_{\text{wet}} - W_{\text{dry}}}{W_{\text{dry}}} \times 100\% \quad (1)$$

2.3.3. Ion-exchange capacity (IEC)

The ion-exchange capacity value was measured by the classical titration technique. Each membrane was placed in 15 ml of 0.05 M sodium chloride aqueous solution for 24 h to exchange the protons with sodium ions. The ion-exchanged (hydrogen chloride) solution was titrated to pH 7.0 with 0.05 M sodium

hydroxide aqueous solution and the end-point was detected with a pH meter (Schott). Three repeated titrations were conducted for each exchanged NaCl solution and the mean titrate volume was used for the IEC calculation.

2.3.4. Proton conductivity

Sample membranes were cut into circular discs of 1.85 cm in diameter, and fully hydrated with deionized water for 24 h prior to measurement. A membrane disc was sandwiched between two aluminum electrodes to form a symmetric test cell. Proton conductivities were measured in the temperature range 30–90 °C after 90 min of equilibration at each temperature, and by electrochemical impedance spectroscopy (EIS) between 1 Hz and 1 MHz on an Eco Chemie PGSTAT 30 poteniostat/galvanostat equipped with a frequency response analyzer module. The proton conductivity of the membrane was calculated with the following formula:

$$\sigma = \frac{L}{RA} \tag{2}$$

where σ, L, R, and A are the proton conductivity, the membrane thickness, the membrane resistance, and the contact area between the electrode and the membrane, respectively. R was taken as the intercept of the complex impedance response (a semicircular arc) on the real axis at the high frequency end [14]. Samples were drawn from at least three different locations in the membrane to obtain an average value of thickness and proton conductivity.

2.3.5. Methanol permeability

Methanol permeability measurements were conducted using a glass diffusion cell. One compartment of the cell ($V_A = 50$ ml) was filled with 2 M methanol solution (8 vol.%, the typical concentration used in current DMFC). The other compartment ($V_B = 50$ ml) was filled with deionized water. The membrane (wetted area = 4.90 cm^2), after being fully hydrated with deionized water for 24 h, was fastened between the two compartments in which the two solutions were kept stirred throughout the measurements. The concentration-driven diffusion of methanol from compartment A to B across the membrane was monitored as a function of time, using a Shimadzu GC2010 gas chromatograph (GC), a HP-Plot Q column (30 m × 0.32 mm × 20 μm), and a flame ionization detector. 1-Butanol was used as an internal standard for the GC measurements.

Under pseudo steady-state conditions which prevailed in the experiments, and for the case $C_B \gg C_A$, the methanol concentration in the receiving compartment as a function of time is given by:

$$C_B(t) = \frac{A}{V_B}\frac{DK}{L}C_A(t - t_0) \tag{3}$$

where C is the methanol concentration; A and L are the membrane area and thickness, respectively; D, K, and t_0 are the methanol diffusivity, solubility, and the measurement time lag, respectively.

The product DK is the membrane permeability. C_B was measured several times during an experiment and the permeability was calculated from the slope of the linear plot of C_B against t, using Eq. (4)

$$\text{slope} = \left(\frac{dC_B(t)}{dt}\right) = \frac{A}{V_B}\frac{DK}{L}C_A$$
$$P = DK = \text{slope} \times \left(\frac{V_B L}{AC_A}\right) \tag{4}$$

The reliability of both the proton conductivity cell and the diffusion cell was checked by measuring the proton conductivity and methanol permeability of Nafion® 117, for which values can be found in the open literature.

2.3.6. Mechanical properties

Mechanical stress–strain measurements were preformed with an Instron Microforce Tensile Tester Machine. Pre-dried membranes were cut into standard dumbbell-shaped test pieces. The two ends of the test piece were clamped on to the tensile machine, and a force of 100 N was pre-applied to compensate for the forces required to straighten the membranes.

3. Results and discussion

3.1. Embedded polymerization-induced membrane structure [15]

Field emission scanning electron microscopy examination of the cross-sections of the AMPS-i (i = 1–5) membranes revealed an asymmetric laminar structure (Fig. 1(a) using AMPS-5 as an example). The three layers in the laminar structure can be differentiated by their differences in texture and morphology. The top and middle layers (Fig. 1(b)) are homogeneous with different morphologies, while the bottom layer (marked as 2) shows greater heterogeneity under high magnification (Fig. 1(c)). According to EDX analysis, the sulfur contents in the three layers decreased in the following order: middle layer > bottom layer > top layer. The hydrophilic network of *P*(AMPS–HEMA–PEGDMA), once formed, will tend to repel the hydrophobic TCPB matrix towards both top and bottom directions, and thereby cause the formation of a tri-layer structure. A small fraction of the hydrophilic network is dragged into the upper layer by the viscous flow of TCPB; and a significantly larger fraction descends into the bottom layer under the influence of the gravitational field. As the cross-linked hydrophilic network becomes less mobile with the progress of polymerization, the bulk of the hydrophilic network is retained in the middle layer. The incompatibility between the hydrophilic network and the hydrophobic TCPB matrix results in phase separation in the bottom layer, as shown by the formation of *P*(AMPS–HEMA–PEGDMA) granules of about 100 nm in size. Phase separation is not apparent in the upper layer because of the lower concentration of the hydrophilic phase.

3.2. Water uptake and ion-exchange capacity (IEC)

The proton conductivity of the PEM is dependent on the number of acid groups in the polymer, their dissociability into

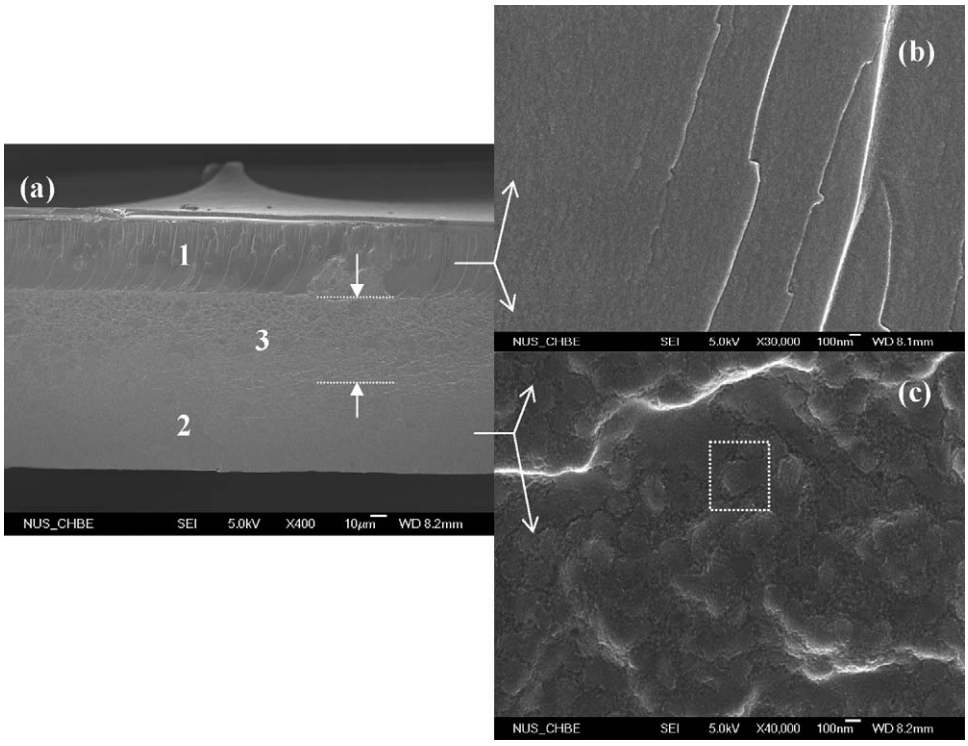

Fig. 1. FESEM cross-section image of AMPS-5 membrane.

protons, and the physicochemical nature of the sites for proton transport [16]. Water molecules attached to the sulfonic acid and hydroxyl groups of the membrane are easily protonated to form hydronium (e.g., H_3O^+, $H_5O_2^+$, etc.) ions. Since proton transport takes place primarily by hopping through the water molecules, a threshold of matrix water is required to maintain proton conductivity. On the other hand, excessive water will result in membrane swelling, mechanical frailty and dimensional changes, all of which will lead to poor performance [17]. The results of water uptake measurements at room temperature are given in Fig. 2 for membranes with different sulfonic acid and HEMA–PEGDMA contents. The membranes were formulated with a hydrophilic HEMA–PEGDMA content in the range of 40–50 wt.%. This seen that water uptake correlates positively with the sulfonic acid group content, but the effect of the HEMA–PEGDMA content on water uptake is only marginal. In order to mitigate the undesirable mechanical properties associated with a high level of water uptake, a denser membrane network is considered to be more suitable. This could, in principle, be achived by substituting PEGDMA with a shorter hydrophilic cross-linkage agent, such as ethylene glycol dimethylacrylate (EGDMA). Experimentally, 10 wt.% of EGDMA in solution B (Table 1) is able to reduce the water uptake to 45%, even at very high sulfonic acid contents (0.70 mmol g^{-1}). The resulting membrane is too brittle, however to be of any practical value. Lowering the EGDMA content restores some of the lost plasticity, but the water reduction properties are unsatisfactory. In short, the water content in the membrane is more dependent on the sulfonic acid content than on the degree of cross-linking.

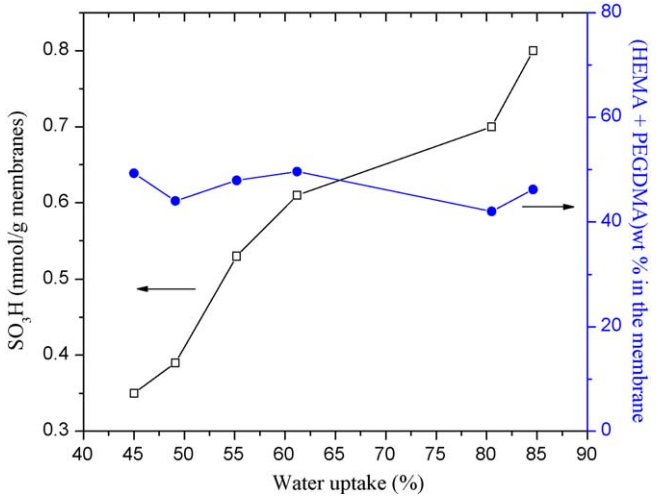

Fig. 2. Effects of sulfonic acid content and (HEMA + PEGDMA) content on water uptake by membranes.

Ion exchange capacity measures the amount of ionizable acid groups in a polymer matrix and results in proton conduction. It is therefore an indirect indicator of proton conductivity. The IEC values of the AMPS-*i* membranes tested in this study are summarized in Fig. 3. Since the sulfonic acid groups are the only ionizable groups in the membranes, the increase in the IEC value with sulfonic acid content is anticipated and easily understood. It has been reported [18] that ionic membranes containing only sulfonic acid groups as the cation-exchange sites exhibit a high level of water uptake, which is also shown in Fig. 3. The IEC values of the AMPS-*i* membranes are lower than the IEC value of Nafion®117 (0.9 meq g^{-1}). It appears that the AMPS groups are not as ionizable as the sulfonic acid groups in Nafion, even in an abundant water environment. The difference can be used

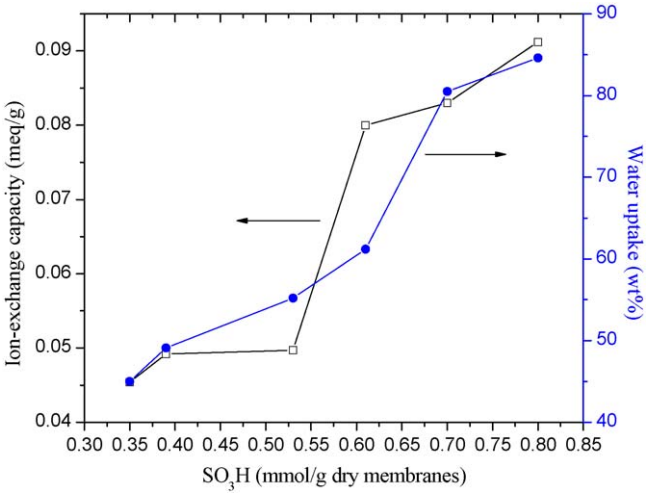

Fig. 3. IEC value and water uptake as a function of sulfonic acid content of membranes.

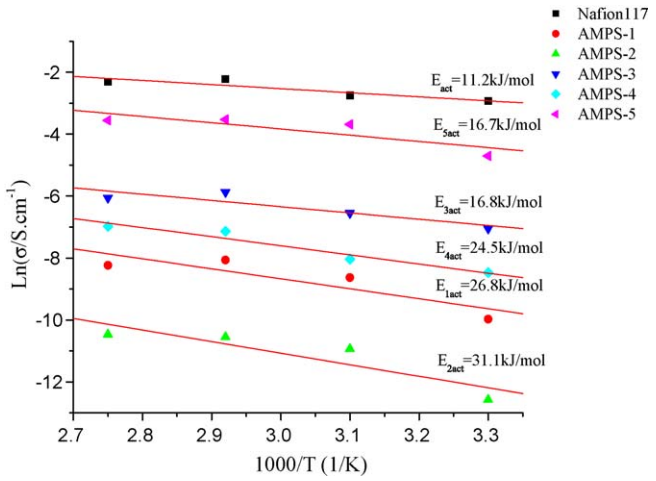

Fig. 5. Logarithm of proton conductivity of AMPS-*i* membranes and Nafion® 117 membrane as function of temperature.

to indicate the influence of the non-charged, methanol-blocking matrix (TCPB)—particularly in the form of a laminar structure with the hydrophilic network sandwiched by two outer layers that consist primarily of TCPB.

3.3. Proton conductivity

The proton conductivities of AMPS-*i* membranes at 70 °C exhibit the expected monotonically increasing trend with sulfonic acid content (Fig. 4). Proton conductivity is highest in AMPS-5 at 0.030 S cm^{-1}, which is of the same order of magnitude as the proton conductivity of Nafion® 117 at the same temperature (0.08 S cm^{-1}).

For the AMPS-*i* ($i = 1$–4) membranes, the presence of dispersed, non-proton conducting segments (Paraloid® resins and PBMA in TCPB) has the net effect of spacing out the sulfonic acid groups, which may account for the slow increase in proton conductivity with sulfonic acid content. The proton conductivity undergoes an abrupt jump in AMPS-5 even though the sulfonic acid content has only been increased incrementally. This could be caused by a sudden increase in the non-freezing water content in AMPS-5. It is known that water in an ionomeric membrane may be partitioned into freezing water and non-freezing water [19]. Non-freezing water is strongly associated with the ionic and polar parts of the polymer, and hence is more crucial to proton conduction. Besides being dependent on the strength of interaction between water and the sulfonic acid groups, the non-freezing water content may also depend on the membrane morphology. The respective contributions are, however, difficult to determine since both factors are also inter-correlated.

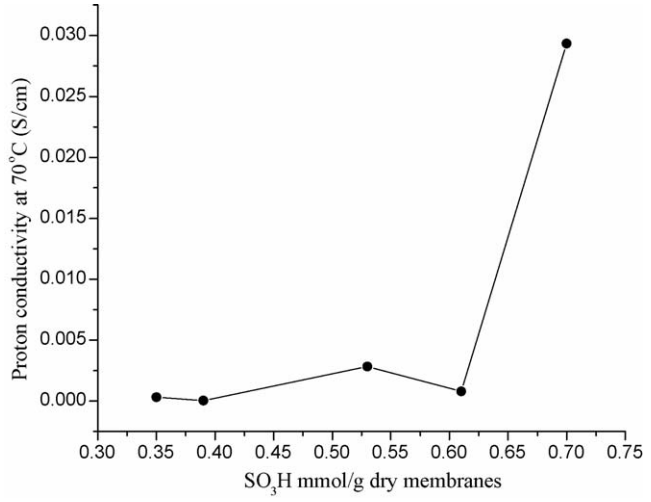

Fig. 4. Proton conductivity of AMPS-*i* membranes at 70 °C.

The Arrhenius plots of proton conductivity for the various AMPS-*i* membranes and the Nafion® 117 membrane are given in Fig. 5. The activation energy deduced from such a plot can often indicate the prevailing mechanism for proton transport. Generally, proton transport in the polymer electrolyte membrane occurs by two mechanisms. In the 'Grotthus' or 'hopping' mechanism, protons are passed down chains of water molecules through many H-bond forming and breaking processes. The water molecules are stationary while protons hop from one water molecule to the other. The Grotthus mechanism is characterized by an activation energy in the range of 14–40 kJ mol^{-1} [20]. The second proton transport mechanism, called the 'vehicle' mechanism, assumes that protons are transported as complexes of the water molecules (e.g., H_3O^+), which are then diffused intact down the concentration gradient. The measured activation energies for the AMPS-*i* membranes are all in the range of 14–40 kJ mol^{-1}, which indicates that proton transport in the AMPS membranes occurs predominantly by the Grotthus mechanism.

3.4. Methanol permeability

The methanol concentration on the receiving side of the diffusion cell was plotted versus time and methanol permeability was determined from the slope according to Eq. (4). The methanol permeabilities of AMPS-*i* membranes at 25 °C and a feed concentration of 2.0 M methanol are shown in

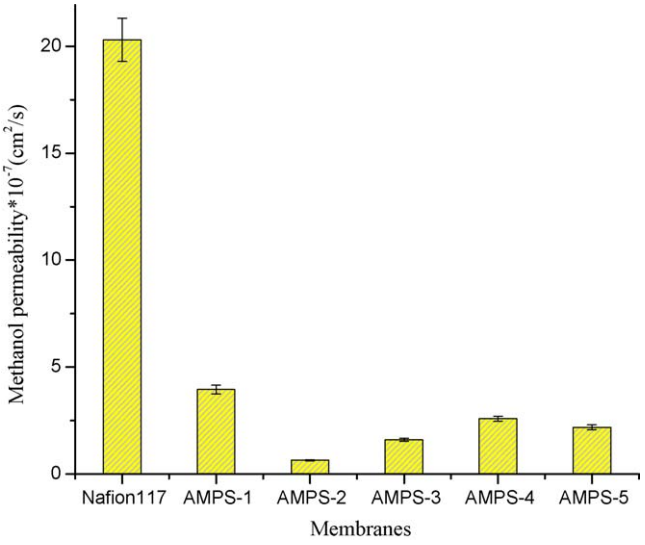

Fig. 6. Methanol permeability of AMPS-*i* membranes.

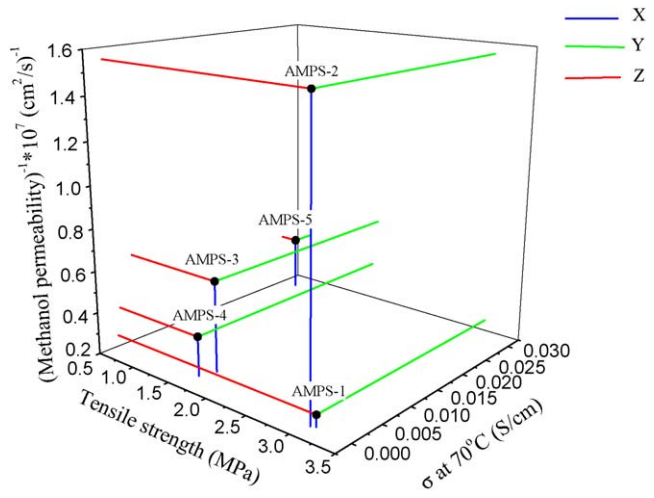

Fig. 7. Three-dimensional graph of AMPS-*i* membranes (tensile strength, proton conductivity at 70 °C and reciprocal of methanol permeability).

Fig. 6. The methanol permeability of Nafion®117 was found to be 1.98×10^{-6} cm^2 s^{-1}, which agrees well with the literature value [21]. The data in Fig. 6 clearly show that the methanol permeabilities of AMPS-*i* membranes are lower than that of Nafion®117. This is particularly true in the case of AMPS-2 for which methanol permeability is more than an order of magnitude lower (about 10^{-8} cm^2 s^{-1}). This result is consequential upon the presence of the methanol-blocking TCPB matrix in the AMPS-*i* membranes. Variations in methanol permeability among the various AMPS-*i* membranes did not, however, follow a systematic trend. Methanol permeability at first decreases and then increases with AMPS content in the membranes. At low AMPS contents, methanol passage is impeded by the association between pendant sulfonic acid groups on different chain segments, which resists swelling. Further increase in the AMPS concentration generally increases membrane hydrophilicity, as methanol can be transported through the water channels.

3.5. Mechanical properties

It is essential for a PEM to have good mechanical integrity to withstand fabrication of the membrane electrode assembly (MEA). The tensile strength at breakdown of the different AMPS-*i* membranes in the dry state is given in Table 2. As a reference, a Nafion®117 membrane was also subjected to the same test. The AMPS-*i* membranes at breakdown are extended considerably, i.e., more than the ultimate elongation of Nafion®117.

Table 2
Tensile strength and elongation of membranes

Membranes	Tensile strength (MPa)	Elongation (%)
AMPS-1	3.10	21
AMPS-2	3.05	16
AMPS-3	1.68	17
AMPS-4	1.62	22
AMPS-5	0.70	14
Nafion®117	2.4	11.8

The results also show a decrease in tensile strength with sulfonic acid content, but the variation of the ultimate elongation with sulfonic acid content for each membrane is less systematic. Weakening of mechanical properties is a known side-effect of sulfonation. The problem is alleviated somewhat through the use of sulfonic monomers compared with the direct sulfonation of polymers. The decrease in the tensile strength may also be attributed to ionic cross-linking in the PEM. Polymer chains in the polyelectrolyte complex that have electrostatic interaction with another polymer chain experience restricted mobility due to ionic cross-linking. This restriction results in an increase in rigidity and thereby reduces the tensile strength.

A three-dimensional plot of the tensile strength, proton conductivity at 70 °C and reciprocal of methanol permeability of the AMPS-*i* membranes is given in Fig. 7. The results show that the properties of the present membranes are still some distant away from their optimum values, i.e., those located in the upper right corner of the diagram.

4. Conclusions

An embedded polymerization scheme is used to fabricate methanol-blocking polymer electrolyte membranes that consist of a methanol-blocking three-component polymer blend of poly(4-vinylphenol-co-methyl methacrylate), poly(butyl methacrylate) and Paraloid® B-82 acrylic copolymer resins, and an embedded proton source of a copolymer of AMPS and HEMA cross-linked by PEGDMA. The embedded polymerization results in an asymmetric membrane structure, in which a hydrophilic network is sandwiched between two layers of predominantly TCPB. The proton conductivities are strongly dependent on the sulfonic acid content and temperature. The proton conductivity of the AMPS-5 membrane at 70 °C is 0.030 S cm^{-1}. The methanol permeabilities of the AMPS-containing membranes are all between 10^{-8} and 10^{-7} cm^2 s^{-1}, and are lower than the methanol permeability of Nafion®117. While the mechanical properties of the AMPS-containing membranes are superior to those of the Nafion®117 membrane, it is

noted that they also exhibit high water uptake and relatively low IEC values. Further improvements are necessary to bring the performance up to the requirements of DMFC applications.

References

[1] J. Sauk, J. Byum, H. Kim, J. Power Sources 132 (2004) 59.
[2] V. Gogel, T. Frey, Y.S. Zhu, K.A. Friedrich, L. Jorissen, J. Garche, J. Power Sources 127 (2004) 172.
[3] C.C. Won, D.K. Ju, I.W. Seong, J. Power Sources 96 (2001) 411.
[4] V. Tricoli, N. Carretta, M. Bartolozzi, J. Electrochem. Soc. 147 (2000) 1286.
[5] Z.G. Shao, I.M. Hsing, Electrochem. Solid State Lett. 5 (2002) A185.
[6] L.J. Hobson, Y. Nakano, H. Ozu, S. Hayase, J. Power Sources 104 (2002) 79.
[7] S.R. Yoon, G.H. Hwang, W.I. Cho, I.H. Oh, S.A. Hong, H.Y. Ha, J. Power Sources 106 (2002) 215.
[8] Y.M. Kim, K.W. Park, J.H. Choi, I.S. Park, Y.E. Sung, Electrochem. Commun. 5 (2003) 571.
[9] Z.G. Shao, X. Wang, I.M. Hsing, J. Membr. Sci. 210 (2002) 147.
[10] M.A. Smit, A.L. Ocampo, M.A. Espinosa-Medina, P.J. Sebastian, J. Power Sources 124 (2003) 59.
[11] Y.C. Si, J.-C Lin, H.R. Kunz, J.M. Fenton, J. Electrochem. Soc. 151 (2004) A463.
[12] B. Yang, A. Manthiram, Eletrochem. Commun. 6 (2004) 231.
[13] C.W. Walker Jr., J. Electrochem. Soc. 151 (2004) A1797.
[14] S.D. Milhailenko, S.M.J. Zaidi, S. Kaliaguine, Catal. Today 67 (2001) 225.
[15] H.Q. Pei, L. Hong, J.Y. Lee, J. Membr. Sci. 270 (2006) 169.
[16] M. Eikerling, A.A. Kornyshev, J. Electroanal. Chem. 502 (2001) 1.
[17] Y. Gao, G.P. Robertson, M.D. Guiver, X. Jian, S.D. Mikhailenko, K. Wang, J. Membr. Sci. 227 (2003) 39.
[18] M.S. Kang, Y.J. Choi, S.H. Moon, J. Membr. Sci. 207 (2002) 157.
[19] D.S. Kim, H.B. Park, J.W. Rhim, Y.M. Lee, Solid State Ionics 176 (2005) 117.
[20] B. Smitha, S. Sridhar, A.A. Khan, Macromolecules 37 (6) (2004) 2233.
[21] Y.A. Elabd, E. Napadensky, J.M. Sloan, D.M. Crawford, C.W. Walker, J. Membr. Sci. 217 (2003) 227.